Ultraviolet Resonance Raman Spectra of Cytochrome *c* Conformational States†

Robert A. Copeland and Thomas G. Spiro*
Department of Chemistry, Princeton University, Princeton, New Jersey 08544
Received January 3, 1985

ABSTRACT: Ultraviolet resonance Raman (UV RR) spectra are reported for ferricytochrome *c* from tuna and horse heart at pH 1.6, 7, 10, and 13, representing distinct conformational states of the protein (states II, III, IV, and V, respectively). The spectra were obtained with pulsed laser excitation at 200 and 218 nm, via H_2 Raman shifting the fourth harmonic output of a pulsed YAG laser. At these deep UV wavelengths, strong enhancement is observed for vibrational modes associated with tryptophan, tyrosine, and phenylalanine side chains and with the amide groups of the polypeptide backbone. The amide I peak frequency is consistent with a dominant contribution from α-helical regions, although a broad high-frequency tail reflects a variety of unordered conformations. The peak frequency is 12 cm^{-1} higher for cytochrome *c* from tuna than from horse, suggesting a less tightly wound structure, which is consistent with the lower denaturation temperature previously reported for the tuna protein. The amide I peak broadens when native protein (state III) is converted to the low- or high-pH forms (states II and IV), reflecting some disordering of the polypeptide chain, but the peak frequencies are unshifted, establishing that the α-helical segments are not completely unfolded in these states. Raising the pH to 13 (state V), however, does produce a frequency upshift, reflecting helix unfolding. The amide II and III frequencies are likewise consistent with a dominant α-helix contribution in the native proteins; they gain intensity, and amide III is shifted to a lower frequency, in states II and IV, consistent with partial disordering. Dissolution of protein in D_2O leads to the disappearance of the amide III band and to a very strong amide II′ band, as recently observed for simple peptides, consistent with stretching of the amide C–N bond in the resonant excited state, and a concentration of the C–N stretching coordinate in the amide II′ mode upon D/H exchange of the amide proton. The tyrosine band intensities change significantly between state III and state II, becoming similar to those displayed by tyrosine itself in water; these changes are attributed to disruption of internal H bonds for two of the four tyrosines (five for tuna) in the protein. Similar, but less marked, changes in the intensity pattern are seen for state IV. In state V, several spectral changes are observed which are consistent with the expected tyrosine ionization at pH 13. Tryptophan modes also show changes in intensity, and in band frequency, suggesting disruption of the internal H bond for the one tryptophan of the horse protein (and one of the two residues in the tuna protein) in states II and V.

Raman spectroscopy has been a valuable tool for the elucidation of protein structural information (Spiro & Gaber, 1977). Visible laser excitation of concentrated protein solutions has been used to obtain Raman data for proteins which do not contain a visible chromophore. When such a chromophore is present, its resonance Raman (RR) spectrum can be obtained with visible laser excitation (Carey, 1982). The unenhanced modes of the protein, however, are suppressed by absorption and cannot be observed. Thus, proteins with visible chromophores have not been amenable to protein conformational studies via Raman spectroscopy with conventional instrumentation.

The advent of reliable ultraviolet lasers makes it possible to study the RR spectra of aromatic amino acid and amide modes in proteins, regardless of the presence of a visible chromophore. Ultraviolet resonance Raman (UV RR) spectra have been reported for aromatic amino acids (Rava & Spiro, 1984, 1985a; Johnson et al., 1984) and for the proteins insulin, α-lactalbumin (Rava & Spiro, 1985b), myoglobin (Johnson et al., 1984), and hemoglobin (Copeland et al., 1985). Excitation at 218 nm gives selective enhancement of tryptophan (Trp) modes, while tyrosine (Tyr) and amide modes are strongly enhanced at 200 nm (Rava & Spiro, 1985a,b,). At 235 nm, both Trp and Tyr modes are seen (Johnson et al., 1984). In the present study, we report RR spectra, with 200- and 218-nm excitation, of ferricytochrome *c* from tuna and horse heart. The conformational states of these two proteins are compared by analysis of the band frequencies and relative intensities of Raman bands associated with amide, tyrosine, phenylalanine, and tryptophan vibrations. For the horse protein, the effects of H/D exchange of the amide and aromatic amino acid residue vibrational modes are also analyzed.

Experimental Procedures

Horse and tuna heart cytochromes *c* were purchased from Sigma and were the highest grades available (the lot assays were 98% and 99% pure, respectively). Solutions of the proteins were prepared in 0.05 M phosphate buffer (pH as indicated in the figure captions) at a concentration of 185 μM. Solutions in D_2O were made in an analogous way. The pD values were corrected for the deuterium isotope effect by adding 0.41 to the pH meter readings obtained (Glasoe & Long, 1960). For Raman intensity measurements, samples of horse heart cytochrome *c* were prepared as above but with 0.2 M ammonium sulfate added as an intensity standard. Tyrosine, tryptophan, and phenylalanine were purchased from Sigma and used as received. Solutions of these amino acids were prepared in H_2O/D_2O containing 0.05 M phosphate buffer (pH/pD 7.0) and 0.2 M ammonium sulfate as an intensity standard for Raman measurements.

Raman spectra were obtained with 200- and 218-nm excitation which was produced by H_2 shifting of the fourth

†This work was supported by National Science Foundation Grant CHE 8106084.

0006-2960/85/0424-4960$01.50/0

harmonic line of a Nd:YAG laser as previously described (Fodor et al., 1985). Raman scattering was collected with 135° backscattering from a flowing (3–5 mL volume, flow rate ~1 mL/s) stream of sample solution. The sample was replaced after each scan (~15 min) to minimize the chance of photodamage to the protein. The Raman collection arrangement and computer interfacing were as previously described (Fodor et al., 1985). Spectra were recorded with 0.05 Å/s increments. The 200-nm spectra are each the sum of 10 consecutive scans (except for the high-pH spectrum of tyrosine which was the sum of 25 scans), while the 218-nm spectra are each the sum of 6 consecutive scans.

To assess the integrity of protein samples after UV Raman spectral acquisition, sodium dodecyl sulfate ($NaDodSO_4$)–polyacrylamide gel electrophoresis was performed on a Bio-Rad Laboratories Protean 16CM apparatus. Slab gels 0.15 cm thick were prepared with 6% polyacrylamide stacking gels (~5 cm long) and 15% polyacrylamide separating gels (~12.5 cm long). Electrophoresis was carried out at a constant 110 V (~30 mA) in the buffer system of Laemmli (1970). The samples were incubated at 100 °C for 5 min in a solution containing 0.5% $NaDodSO_4$ and 5% 2-mercaptoethanol, before electrophoresis. The gels were stained with Vesterberg's (1971) preparation and destained with acetic acid/ethanol/water (7.5:10:82.5 by volume). Samples of horse cytochrome *c* (state III) before and after UV irradiation gave identical results upon electrophoresis.

The samples were also checked for laser-induced damage by UV–vis absorption spectroscopy after the Raman spectra were recorded, using a Hewlett-Packard 8450A diode array UV–vis spectrophotometer. No evidence of laser damage was observed. At pH 7, the weak 695-nm absorption band of ferricytochrome *c* is known to be a marker of conformational integrity and the presence of an intact Met-80–iron bond (Dickerson & Timkovick, 1975). Careful examination of this spectral region before and after laser irradiation for state III ferricytochrome *c* indicated that no disruption of this bond had occurred, even after extensive irradiation.

Far-ultraviolet absorption spectra were taken on a Cary 14 UV–vis spectrophotometer. The conditions for spectral acquisition are described in the caption of Figure 10.

A functional assay with cytochrome oxidase [bovine, prepared by the method of Yoshikawa et al. (1977)] was carried out (Wharton & Tzagoloff, 1967). Rates of electron transfer were determined spectrophotometrically from the slopes of log $(A_0/A_t)_{550nm}$ vs. time plots. The mean slope values were 3.4 $\times 10^{-2} \pm 5 \times 10^{-3}$ and $3.5 \times 10^{-2} \pm 1 \times 10^{-3}$ min^{-1} before and after Raman irradiation, respectively (mean of three runs per sample, all plots gave correlation coefficients which were significant at >99% confidence level). Thus, no loss of electron-transfer ability resulted from the UV exposure experienced by samples during Raman spectral acquisition. However, prolonged exposure (>1.5 h) to UV laser pulses did significantly reduce the electron-transfer rates, even though no change in the absorption spectrum was observed. Since the reaction of cytochrome *c* with cytochrome oxidase is abolished when certain surface lysine residues are chemically modified (Dickerson & Timkovich, 1975), we speculate that one or more of these lysine residues may be damaged by prolonged UV irradiation; it may be relevant that ammonia molecules have been reported to degrade under similar conditions (Ziegler & Hudson, 1984).

Results

UV RR spectra have been obtained for cytochrome *c* from horse and tuna with excitation at 200 nm (Figures 1 and 2)

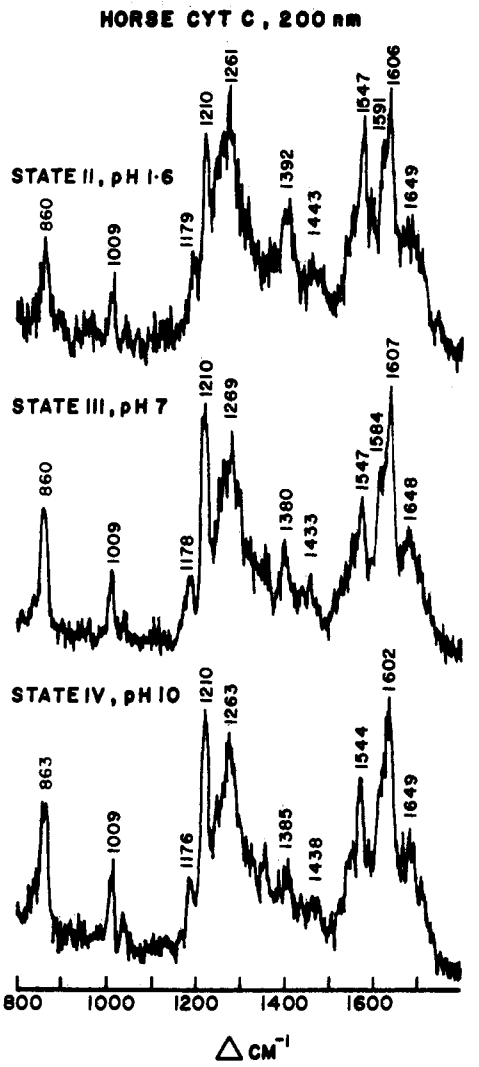

FIGURE 1: Resonance Raman spectra of horse heart cytochrome *c* with 200-nm excitation. From top to bottom: state II, pH 1.6; state III, pH 7.0; and state IV, pH 10.0.

and 218 nm (Figures 3 and 4). Ferricytochrome *c* exists in five reversible, pH-dependent conformational states with pK_a's of 0.42, 2.50, 9.35, and 12.76, which have been labeled states I, II, III, IV, and V, respectively (Dickerson & Timkovick, 1975). Four of these states, II–V, have been included in this study, as indicated in the figures. The visible absorption spectra for the samples were in quantitative agreement with those reported in the literature (Theorell & Åkerson, 1941). In the ultraviolet region, absorption from the amide chromophores and aromtic side chains is observed, and at pH 13 (state V), hydroxide absorbs strongly toward 200 nm so that acquisition of RR spectra at this wavelength was difficult. At these deep UV wavelengths, all of the Raman bands are assignable to the aromtic side chains of phenylalanine, tyrosine, and tryptophan and to bands associated with the amide groups of the polypeptide main chain (Rava & Spiro, 1985b). The observed band frequencies and their assignments are given in Tables I and II.

The amide vibrations, I, II, and III, are seen at 200 nm but not at 218 nm. Their frequencies are ~1650, ~1550, and ~1265 cm^{-1}. The amide II band is very weak in nonresonance Raman spectra recorded with visible excitation but has been shown to undergo preresonance enhancement in 257.3-nm Raman spectra of peptides (Harada et al., 1975; Sugawara et al., 1978); it is strongly enhanced at 200 nm (Rava & Spiro, 1985). When the amide NH proton is exchanged with a

Table I: RR Band Frequencies (in cm^{-1}) and Assignments for Cytochrome *c* with 200-nm Excitation

state II, pH 1.6		state III, pH 7.0		state IV, pH 10.0		
horse	tuna	horse	tuna	horse	tuna	assignment[a]
1649	1661	1648	1659	1649	1662	amide I
1606	1612	1607	1614	1602	1613	Tyr + Phe
1591	1598 (sh)[b]	1584	1592	–	1596 (sh)	Phe
1547	1550	1547	1550	1544	1555	amide II
1443	1450	1433	–[c]	1438	–	CH_2 bend
1392	1388	1380	1380	1385	1383	CH_2 bend
1261	1258	1269	1268	1263	1264	Tyr + amide III
1210	1209	1210	1206	1210	1206	Tyr
1179	1175	1178	1178	1176	1177	Tyr
1009	1000	1009	1006	1009	1006	Phe
860	850	860	853	863	853	Tyr

[a] Assignments based on data from Rava & Spiro (1985a,b). [b] sh, shoulder. [c] Band not observed.

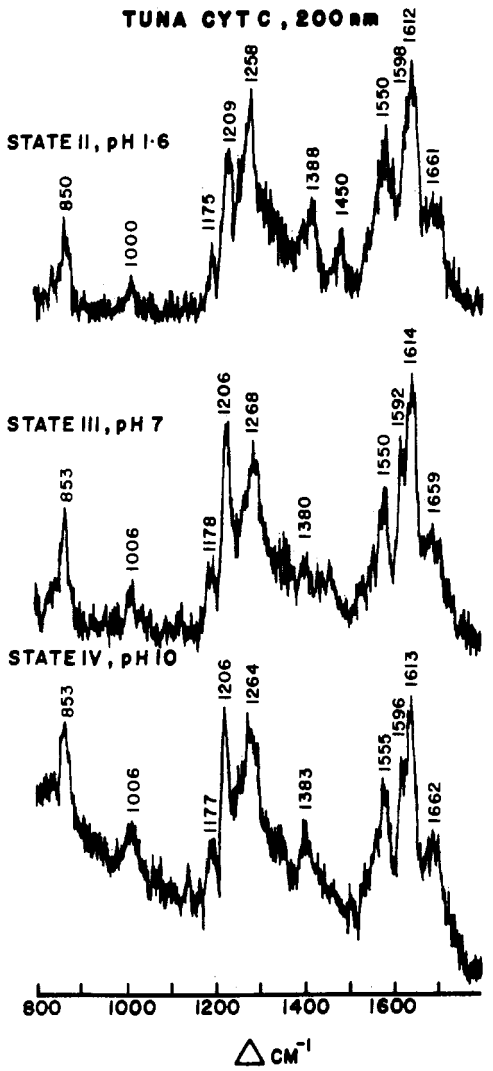

FIGURE 2: Resonance Raman spectra of tuna heart cytochrome *c* with 200-nm excitation. From top to bottom: state II, pH 1.6; state III, pH 7.0; and state IV, pH 10.0.

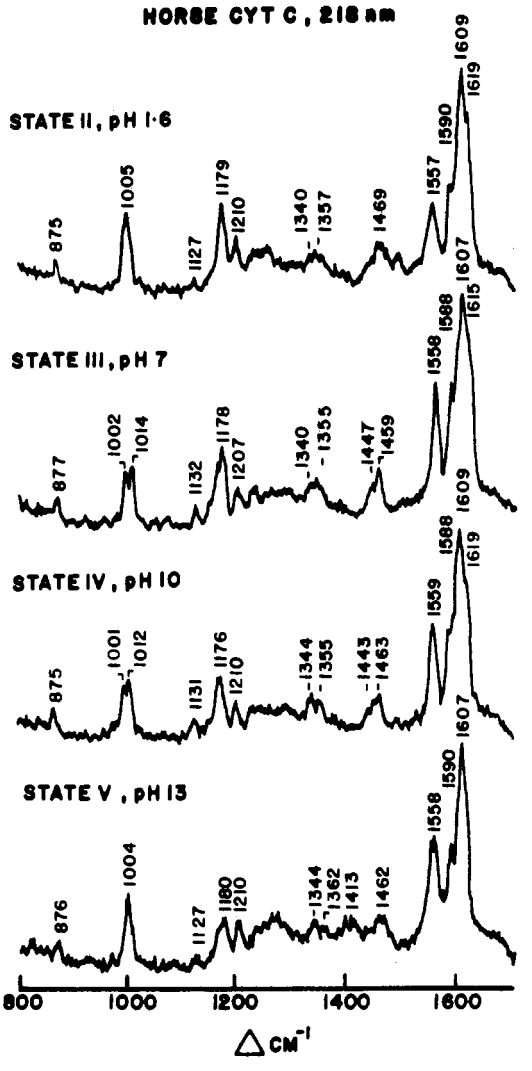

FIGURE 3: Resonance Raman spectra of horse heart cytochrome *c* with 218-nm excitation. From top to bottom: state II, pH 1.6; state III, pH 7.0; state IV, pH 10.0; and state V, pH 13.0.

deuteron, the amide II and III vibrations (now labeled II′ and III′) are shifted to ~1465 and ~1005 cm^{-1} (Sugawara et al., 1978). When cytochrome *c* is dissolved in D_2O, a very strong amide II′ band at ~1465 cm^{-1} is seen with 200-nm excitation and retains moderate intensity with 218-nm excitation (Figures 5 and 6), but no amide III′ band is seen. Similar results have recently been reported (Hudson & Mayne, 1984) for *N*-methylacetamide and attributed to amide C–N bond stretching in the resonant $\pi-\pi^*$ electronic transition (186 nm). The amide II and III modes are mixtures of C–N stretching and N–H bending, but replacement of H by D on N greatly lowers the natural frequency for N–H bending, leaving amide II′ with mostly C–N stretching character and amide III′ with mostly N–D bending character. Thus, the resonance enhancement is concentrated in amide II′ following D/H exchange of the amide proton.

The remaining bands in the 200-nm spectra are assignable to tyrosine and phenylalanine modes, although there are unassigned bands at ~1380 and ~1440 cm^{-1}, which may be due to CH_2 bending vibrations (Frushour & Koenig, 1975). Tryptophan bands are not seen at 200 nm. They are known (Rava & Spiro, 1984, 1985a) to be substantially weaker at

Table II: RR Band Frequencies (in cm^{-1}) and Assignments for Cytochrome *c* with 218-nm Excitation

state II, pH 1.6		state III, pH 7.0		state IV, pH 10.0		state V, pH 13.0		
horse	tuna	horse	tuna	horse	tuna	horse	tuna	assignment[a]
1619	–	1615	1616	1619	1617	–	–	Trp + Tyr
1609	1608	1607	1606	1609	1602	1607	1604	Phe + Tyr
1590	–	1588	–	1588	1586[b]	1590	1590	Phe
1557	1558	1558	1559	1559	1556	1558	1556	Trp
1469	1463	1459	1461	1463	1456	1462	1459	Trp + CH_2 bend
–[c]	–	1447	–	1443	–	–	–	CH_2 bend
–	–	–	–	–	1412	1413	1412	ν_{COO^-} sym.[d] or ν_{19b} Tyr
1357	1358	1355	1354	1355	1361	1362	1363	Trp
1340	1343	1340	1340	1344	1345	1344	1350	Trp
1210	1206	1207	1206	1210	1206	1210	1208	Tyr
1179	1175	1178	1178	1176	1177	1180	1177	Tyr
1127	–	1132	1133	1131	1127	1127	1126	?
–	1009	1014	1013	1012	1010	–	1009	Trp
1005	–	1002	–	1001	–	1004	–	Phe
875	879	877	881	875	876	876	880	Trp

[a] Assignments based on data from Rava & Spiro (1985a,b). [b] Shoulder. [c] Band not observed. [d] sym., symmetric.

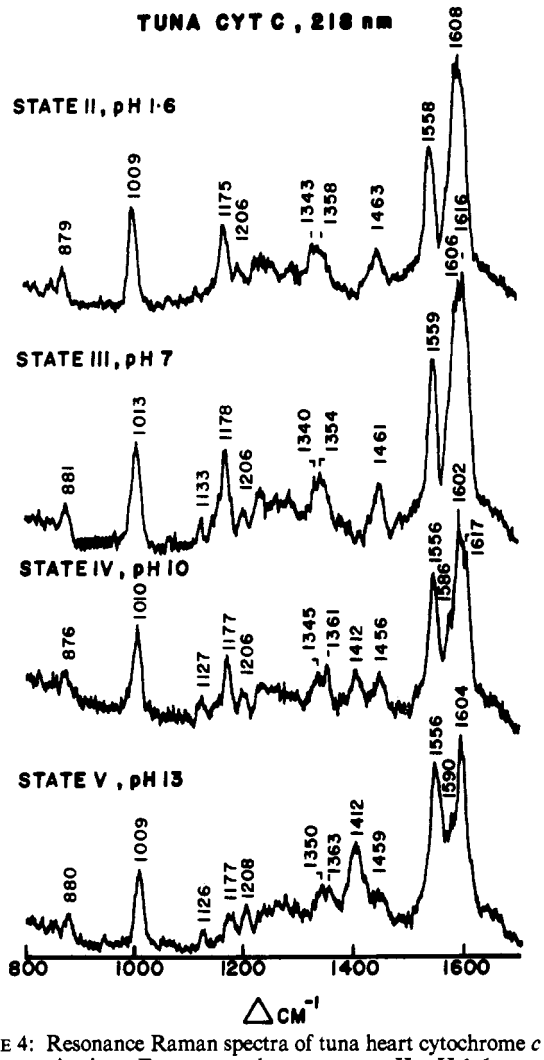

FIGURE 4: Resonance Raman spectra of tuna heart cytochrome *c* with 218-nm excitation. From top to bottom: state II, pH 1.6; state III, pH 7.0; state IV, pH 10.0; and state V, pH 13.0.

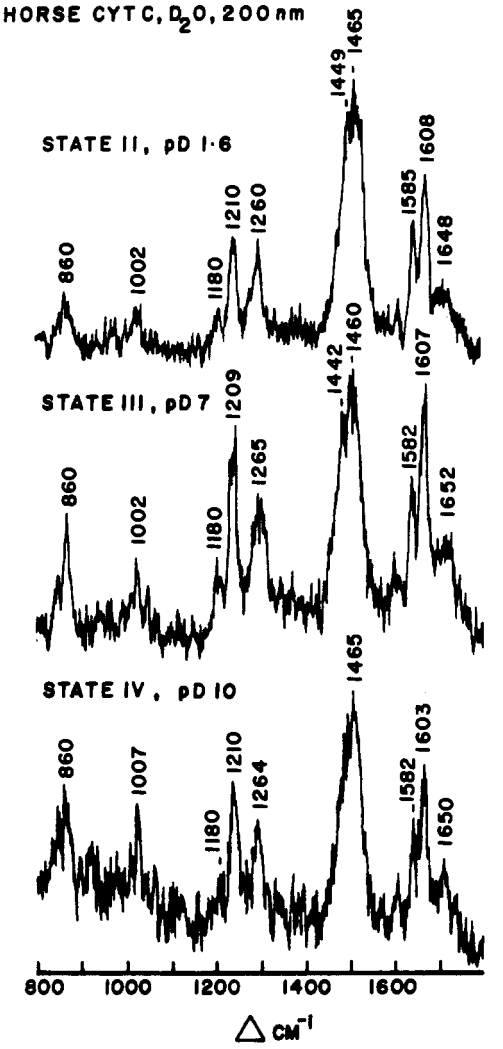

FIGURE 5: Resonance Raman spectra of horse heart cytochrome *c* in D_2O with 200-nm excitation. From top to bottom: state II, pD 1.6; state III, pD 7.0; state IV, pD 10.0.

this wavelength than for tyrosine and phenylalanine, even though the tryptophan absorption is quite strong. This phenomenon, which may be associated with spectral congestion of electronic states, has been discussed elsewhere (Rava & Spiro, 1985a). Tyr shows isolated bands at ~850, ~1178, and ~1210 cm^{-1}, while Phe shows an isolated band (the benzene ring breathing mode, ν_1) at ~1005 cm^{-1}. Cytochrome *c* from tuna contains five Tyr and three Phe, while that from horse contains four each of Tyr and Phe. This change in the Phe/Tyr ratio from 0.6 to 1.0 is readily apparent in the relative intensities of the Tyr and Phe bands in the 200-nm spectrum. The doublet at ~1610, 1590 cm^{-1} is due to overlapping contributions from ring modes ν_{8a} and ν_{8b} of Tyr and Phe, which are seen (Rava & Spiro, 1985a) at 1617, 1601 cm^{-1} and 1606, 1586 cm^{-1}, respectively, in the spectra of the amino acids themselves. This doublet is higher in frequency for tuna than for horse cytochrome *c*, reflecting the lower Phe/Tyr ratio.

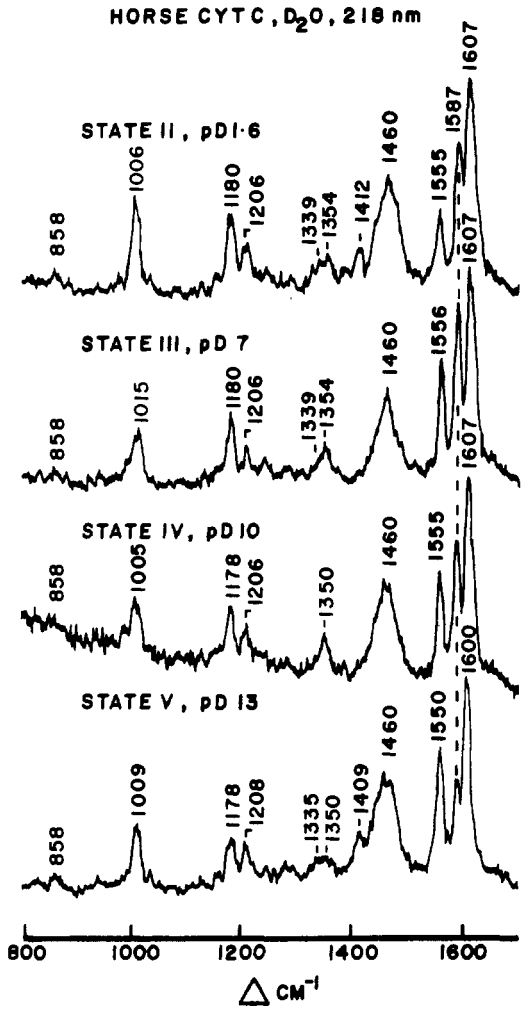

FIGURE 6: Resonance Raman spectra of horse heart cytochrome *c* in D_2O with 218-nm excitation. From top to bottom: state II, pD 1.6; state III, pD 7.0; state IV, pD 10.0; and state V, pD 13.0.

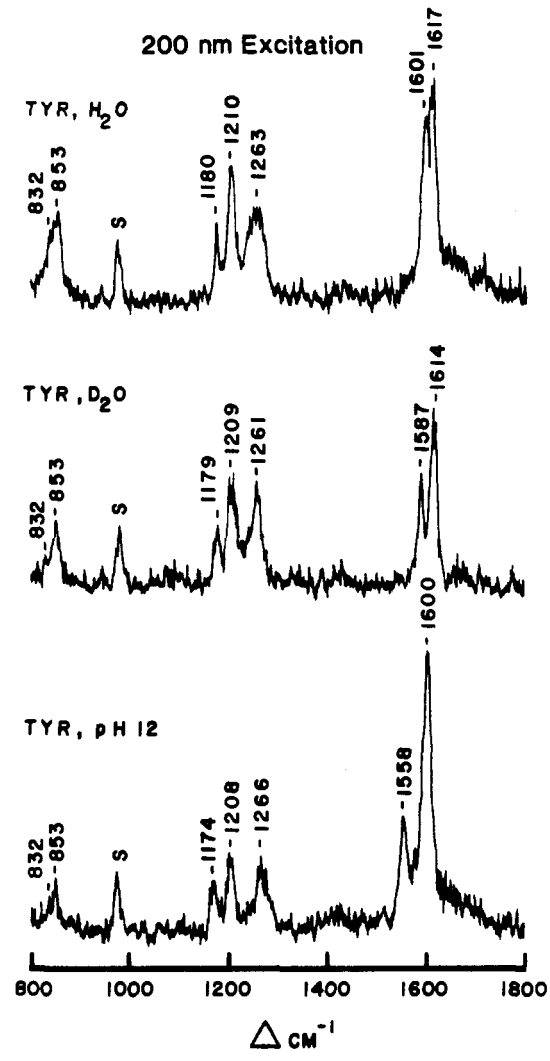

FIGURE 7: Resonance Raman spectra of tyrosine with 200-nm excitation. From top to bottom: H_2O, pH 7.0; D_2O, pD 7.0; and H_2O, pH 12.0. The band marked "S" is due to sulfate (981 cm^{-1}) which was added as an intensity standard.

At 218 nm, which is coincident with the first allowed $\pi-\pi^*$ transition of tryptohan, strong enhancement of Trp modes is observed. Isolated Trp bands are found at ~875, 1345, 1360, and 1555 cm^{-1}. The ~1460 cm^{-1} Trp mode has a low-frequency shoulder, which may be associated with the CH_2 bending mode, also observed at 200 nm. The ν_{8a}, ν_{8b} doublet of Phe/Tyr remains strong at 218 nm due to enhancement via a vibronic coupling mechanism (Rava & Spiro, 1985a) but also encompasses a weak contribution from the 1620 cm^{-1} Trp mode. Other Tyr contributions can be seen at ~1180 and 1210 cm^{-1}. Likewise, the Phe 1005 cm^{-1} band is detectable, next to the Trp band at ~1015 cm^{-1}. A doublet is seen clearly in this region for states III and IV of horse cytochrome *c*, which contains only one Trp, for a Phe/Trp ratio of 4. Tuna cytochrome *c*, however, contains two Trp and has a Phe/Trp ratio of 1.5; only a single band can be observed, with a frequency close to that of Trp itself (Figure 4).

In addition to the amide N–H protons, there are exchangeable protons on Tyr (OH) and Trp (indole NH). As shown in Figures 7 and 8, the effect on the Tyr 200- and 218-nm RR spectrum of exchanging D_2O for H_2O is limited to downshifts in the ν_{8a} and ν_{8b} bands by 3 and 14 cm^{-1}, to 1614 and 1587 cm^{-1}. The ν_{8b} downshift is detectable for horse cytochrome *c* in D_2O (Figure 5), where the ~1585 cm^{-1} component of the Phe/Tyr doublet is better resolved than in H_2O (Figure 1). Also shown in Figures 7 and 8 is the RR spectrum of tyrosinate, for which the ν_{8a}, ν_{8b} doublet shifts to 1600, 1558 cm^{-1}. The 218-nm RR spectra of cytochrome *c* at pH 13 appear to show increased intensity in the ~1558 cm^{-1} region, reflecting ionization of the tyrosines (at 218 nm, this region is also occupied by a strong Trp mode, vide infra). Figure 9 shows the effect on the Trp 218-nm spectrum of dissolution in D_2O. Several small changes in frequency and/or intensity can be seen, of which the 20 cm^{-1} downshift of the 880 cm^{-1} band is the most pronounced. We have ascertained that the shift in the 1622 cm^{-1} band to 1613 cm^{-1} is time dependent and is attributable to laser-induced D/H exchange at the C_4 position of the indole ring (Saito et al., 1984). Comparing the horse cytochrome *c* 218-nm spectra in D_2O (Figure 6) and H_2O (Figure 3), we see that the 880 cm^{-1} band has shifted down to 860 cm^{-1} due to exchange of the indole NH proton. Figure 9 also shows that only slight effects are observed in the RR spectrum of Trp upon ionization of the indole NH proton at pH 13. As reported under Experimental Procedures, cytochrome *c* retained its integrity during acquisition of the UV RR spectra, as judged by the absorption spectrum and functional assay, although prolonged UV irradiation was found to diminish electron-transfer activity to cytochrome oxidase.

Discussion

Cytochrome *c* is a small [~13 kilodaltons (kDa)] soluble heme protein which serves to shuttle electrons between cyto-

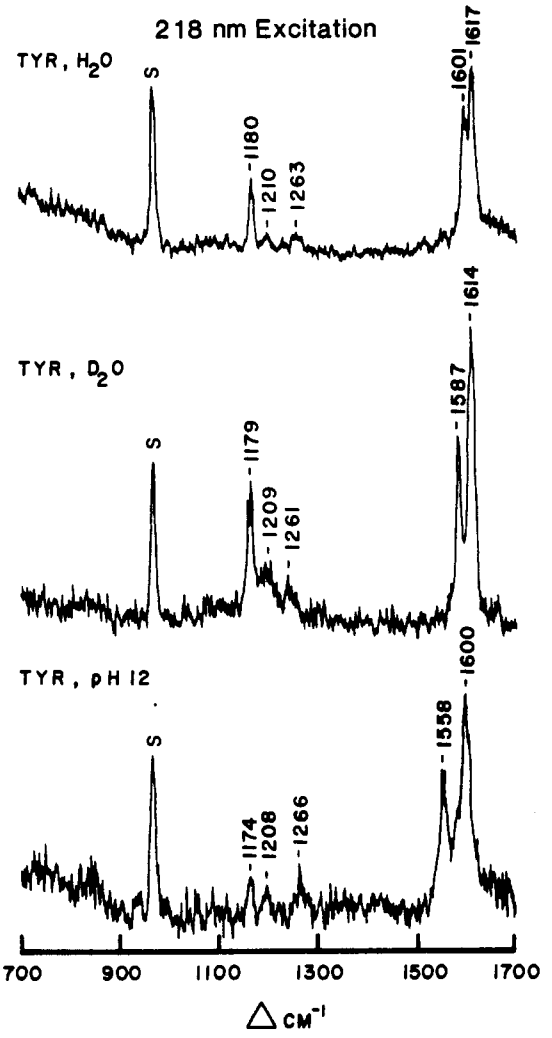

FIGURE 8: Resonance Raman spectra of tyrosine with 218-nm excitation. From top to bottom: H_2O, pH 7.0; D_2O, pD 7.0; and H_2O, pH 12.0. The band marked "S" is due to sulfate (981 cm^{-1}) which was added as an intensity standard.

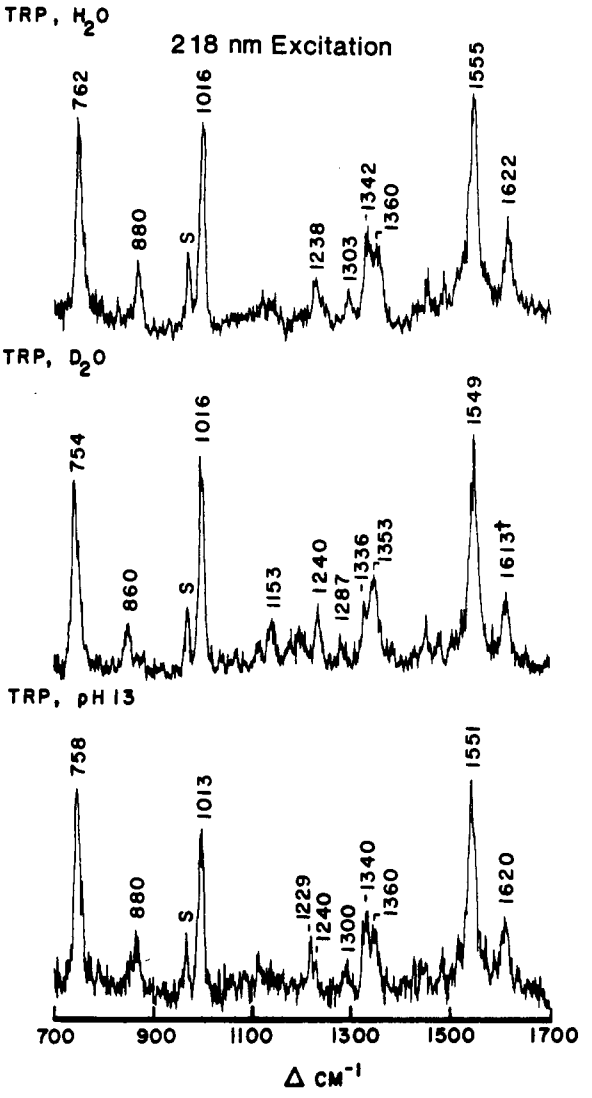

FIGURE 9: Resonance Raman spectra of tryptophan with 218-nm excitation. From top to bottom: H_2O, pH 7.0; D_2O, pD 7.0; and H_2O, pH 13.0. The band marked "S" is due to sulfate (981 cm^{-1}) which was added as an intensity standard. The shift of the 1622 cm^{-1} band to 1613 cm^{-1} in D_2O (†) is due to a photoinduced H/D exchange of the C_4 proton (see text).

chrome reductase and cytochrome oxidase in the respiratory electron-transfer chain (Dickerson & Timkovick, 1975). Crystal structures have been carried out for the two proteins included in the study, from tuna and horse heart (Dickerson et al., 1971; Swanson et al., 1977). They show very similar tertiary structures. The polypeptide chain forms five sections of α helix, residues 1–11, 49–55, 60–68, 70–75, and 89–101, and no β sheet (Takano et al., 1977). The prosthetic group is protoheme covalently linked to the polypeptide chain via condensation of its vinyl peripheral substitutents with cysteinal side chains. The heme iron atom has imidazole and thioether axial ligands, the side chains of His-18 and Met-80, and is low spin. In the Fe^{III} form (ferricytochrome *c*), Met-80 is replaced by another ligand, possibly Lys-79 or -72 (Dickerson & Timkovick, 1975), when the pH is raised from neutrality, with a transition pK_a of 9.35; this form is also low spin. The ligation change must be accompanied by a conformational rearrangement of the protein. The interconversion of the two protein conformations in the reduced form of the protein has a time constant of ~100 ms, as judged by the relaxation of the spectral intermediate produced by rapid reduction of the alkaline form of ferricytochrome *c* (Lambeth et al., 1973; Land et al., 1971, 1974). Raising the pH of the Fe^{III} form to 13 produces yet another low-spin state (V) with a shifted Soret absorption band; considerable unfolding of the protein is believed to take place at this high pH (Dickerson & Timkovick, 1975). Lowering the pH of the neutral form (state III) leads to the production of high-spin heme, with a pK_a of 2.5 (state II), in which at least one of the axial ligands has presumably been replaced by a water molecule. Further acidification (pK_a = 0.42) produces another high-spin form (state I), in which the protein is believed to be largely denatured (Dickerson & Timkovick, 1975).

Amide Bands. The frequency of the amide I mode, which is largely C=O stretching in character, is known to be sensitive to the peptide conformtion. In nonresonant Raman spectra (Williams, 1983; Carey, 1982), this frequency is lowest, 1645–1660 cm^{-1}, for α-helical structures and highest, 1665–1680 cm^{-1}, for β-sheet structures, with "unordered" segments having intermediate values, 1660–1670 cm^{-1}. All of our 200-nm spectra show amide I bands peaking at 1645–1660 cm^{-1}, in the α-helix range, but they show broad tails toward the high-frequency side, consistent with a distribution of unordered conformations in the extensive nonhelical regions of the cytochrome *c* backbone. Interestingly, however, the peak frequency for the horse protein is consistently ~12 cm^{-1} lower than for the tuna protein. The tertiary structures for the two proteins are believed to be quite similar,

although the crystal structure of the horse protein has only been carried to a resolution of 2.8 Å, which is insufficient for detailed conformational analysis (Dickerson et al., 1971). Nevertheless, there are clearly some structural differences between the two proteins, since the denaturation temperature for the horse protein is at least 10 °C higher than that of the tuna protein (Moore & Williams, 1980). The differences in denaturation temperature and in the amide I frequency are both suggestive of a higher content of regular α helix for the horse protein. For both proteins, the amide I band is sharpest at neutral pH (state III) and broadens noticeably at high and low pH (states IV and II). This behavior is consistent with some disordering of the peptide backbone in these states. Nevertheless, the peak frequencies do not change significantly, indicating that the α-helical segments are largely intact in all three states. This is a significant observation, since previous studies have indicated a substantial protein unfolding below pH 2 (Wooten et al., 1981; Drew & Dickerson, 1978; Babul & Stellwagen, 1972). Although state II is commonly assumed to have a random-coil structure, the RR spectra clearly show that this description is inaccurate; likewise, there is ^{13}C NMR evidence (Schejter et al., 1978; Cohen & Hayes, 1974) that the tertiary structure of the protein is maintained to a large degree, below pH 2. At pH 13 (state V), however, the amide I band was observed to broaden markedly, and the peak frequency shifted to 1670 cm^{-1}, consistent with substantial unfolding of the helixes.

The amide II band has been studied in infrared spectra, where it shows up strongly, and is found to occur at ~1550 cm^{-1}, largely independent of peptide conformation (Suzuki et al., 1966). Likewise, the frequency varies only slightly in the 200-nm RR spectra of cytochrome *c* (Figures 1 and 2). However, its intensity is higher, relative to the amide I band (or the nearby ν_{8a}, ν_{8b} Phe/Tyr doublet), in states II and IV than in state III. The same effect can be seen for the amide II′ band in D_2O solution (Figure 5). In state V (pH 13), the trend continues with even higher relative intensity for amide II. This behavior suggests that the amide II intensity is higher for unordered segments than for α helixes. We attribute this behavior to Raman hypochromism associated with the known (Rosenheck & Doty, 1961) absorption hypochromism of the resonant 190-nm amide absorption band which is associated with the alignment of the transition dipoles in α helixes. Figure 10 shows that the 190-nm absorbance does increase between state III and states II and IV, as expected for partial unfolding of the α helixes. Both the 190-nm absorption and the amide II Raman intensity indicate a greater loss of helical content in state II than in state IV.

The amide III band, at ~1265 cm^{-1}, is obscured by overlap with a tyrosine band at the same frequency (Frushour & Koenig, 1975; Rava & Spiro, 1985). Comparison with the spectra taken in D_2O (Figure 5) shows that tyrosine in fact accounts for most of the intensity in this band. In nonresonance Raman spectra, the amide III band is broad (1265–1300 cm^{-1}) and quite weak for α helixes. It intensifies and shifts down in frequency for β-sheet (1230–1240 cm^{-1}) and unordered (1240–1260 cm^{-1}) segments. It is therefore significant that the 1269 cm^{-1} band of state III (pH 7) shifts down by ~10 cm^{-1} and becomes substantially stronger in state II (pH 1.6) consistent with an augmented contribution from unordered segments.

Tyrosine. Comparing the 200-nm spectrum of tyrosine in D_2O with that of horse cytochrome *c* in D_2O (Figures 7 and 5), we see that the trio of bands at 1180, 1210, and 1260 cm^{-1} has the same relative intensity for state II, but in states III and IV, the 1210 cm^{-1} band is significantly stronger. A similar trend is evident in H_2O, although the 1260 cm^{-1} band is overlapped by amide III. The horse protein has two Tyr residues (74 and 97) which are exposed to the solvent and two (48 and 67) which are buried and involved in H bonding, one of them (48) to the propionate peripheral substituent of the heme. The RR spectra strongly suggest that these internal H bonds are broken and the tyrosines exposed to solvent in state II. A similar exposure to solvent is seen for a bruied, H-bonded Trp residue (vide infra) in state II. Tyrosine (67) and Trp (59) are at the ends of the middle α-helical segment (60–68) of the polypeptide chain. Movement of this segment relative to the rest of the protein is suggested for the state III → state II transition.

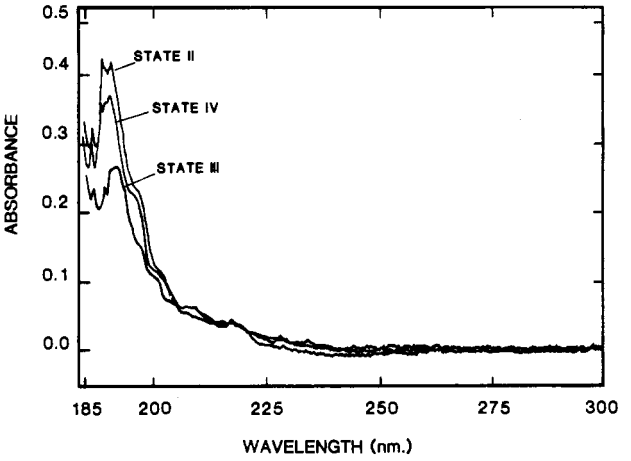

FIGURE 10: Far-ultraviolet absorption spectra of horse ferricytochrome *c* at various pHs. Spectra were recorded on a nitrogen-purged (~5 h) Cary 14 UV–vis spectrophotometer. Samples were 185 μM cytochrome *c* in 0.05 M phosphate buffer (state II, pH 1.6; state III, pH 7.0; state IV, pH 10.0) contained in 0.1-mm fused silica cuvettes and were run with the appropriate buffer solutions in the reference cell.

Clear indications of tyrosine ionization in state V (pH 13) are seen in the 218-nm spectra by comparison with the 218-nm RR spectra of tyrosine and tyrosinate (Figure 9). The shift in Tyr ν_{8a}, ν_{8b} from 1614, 1601 to 1600, 1558 cm^{-1} produces a narrowing of the 1604 cm^{-1} band (Phe + tyrosinate) and an augmentation of the 1556 cm^{-1} band (Trp + tyrosinate). There is also a marked decrease in relative intensity for the 1178 cm^{-1} Tyr band, similar to that observed on tyrosine ionization (Figure 9). The 1180 cm^{-1} band diminution is much more marked at 218 than at 200 nm, presumably reflecting altered resonance conditions with respect to the tyrosinate electronic transition frequencies.

We note that the 860 cm^{-1} Tyr band in the 200-nm spectra of horse cytochrome *c* is stronger and sharper in state III than in state II. This effect may be linked to the internal H-bond effects noted above. The broadening of the 860 cm^{-1} band in state II is no doubt associated with development of an 830 cm^{-1} shoulder, associated with the Fermi doublet of tyrosine, which has been much studied via nonresonance Raman spectroscopy (Siamwiza et al., 1975; Carey, 1982). The relative intensities of the 830, 860 cm^{-1} components of this doublet are known to be influenced by the state of tyrosine H bonding (Siamwiza et al., 1975). The 200-nm spectrum of tyrosine itself (Figure 5) shows a prominent 832 cm^{-1} shoulder. It is plausible that diminution of this shoulder for the two tyrosines which are buried and internally H bonded in state III is responsible for the apparent sharpening and intensification of the 860 cm^{-1} band. The frequency of this band is several wavenumbers higher for protein from horse

than from tuna, or for tyrosine itself in H_2O. The tuna protein has an extra Tyr (46), which is H bonded to the backbone carbonyl of Val-28 (Dickerson & Timkovick, 1975), which might account for an apparent downshift of the composite band. Alternatively, the less "tightly wound" polypeptide structure which is suggested by the higher amide I peak frequency for tuna cytochrome *c* might weaken the Tyr internal H bonds and produce an average frequency for the ring breathing mode that is closer to the observed value for tyrosine in water.

Tryptophan. In an UV RR study of α-lactalbumin (Rava & Spiro, 1985b), it was possible to associate the exposure of tryptophan residues with specific changes in the 218-nm spectrum, especially a shift in intensity from the ~1360 to the ~1350 cm^{-1} band, and a 4 cm^{-1} frequency upshift of the 876 cm^{-1} band. In the 218-nm spectra of horse and tuna cytochrome *c* (Figures 3 and 4), the 1345, 1360 cm^{-1} bands are weak and poorly resolved, but there does seem to be an intensification of the former relative to the latter on going from state III to state II or IV; there is also a slight (2 cm^{-1}) but consistent downshift of the ~880 cm^{-1} band. More noticeable effects are seen for the 1559 cm^{-1} band, which shows a higher relative intensity for state III than for state II or IV, and for the 1014 cm^{-1} band, which loses intensity in states II, IV, and V relative to state III, thus causing the apparent downshift of the composite Tyr/Phe band at ~1009 cm^{-1}. These systematic changes must reflect alterations in the average tryptophan environment. The horse protein has only a single Trp, and it is H bonded to a heme propionate group. In view of the results obtained for tyrosine, it is plausible that this H bond is disrupted in states II and V, and perhaps state IV, producing the observed spectral alterations. The tuna protein contains a second Trp, which is exposed to solvent and probably does not contribute to the spectral changes. This additional Trp may account for the slight upshift and broadening of the 880 cm^{-1} band in tuna relative to horse cytochrome *c*.

Conclusions

The UV RR band frequencies and intensities of cytochrome *c* allow the following inferences to be made about its tertiary structure. (1) The amide I peak frequency shows the RR scattering from the collection of C=O bond stretches to be dominated by the α-helical regions of the protein, although the high-frequency tail reflects a range of unordered conformations. Interestingly, the peak frequency is ~12 cm^{-1} higher for tuna than for horse cytochrome *c*, suggesting less helical content for the former, consistent with the lower denaturation temperature for the tuna protein. At pH 1.6 and 10 (states II and IV), the proteins show broadening of the amide I band, indicating some disordering of the backbone, but the peak frequency remains unchanged, demonstrating significant retention of the α-helical regions. Some unfolding is nevertheless evident from the intensification of the amide II and III bands (and a shift to lower frequency of the latter) in parallel with the 190-nm absorption intensity increase due to the loss of hypochromism associated with the α-helix structure. At pH 13 (state V), complete unfolding is seen. (2) Alterations in tyrosine band intensities show evidence for disruption of internal H bonds in state II, whose tyrosine intensities are similar to those shown by tyrosine itself in water. The intensity changes for state IV are in the same direction, but are less marked. State V shows clear spectral evidence for tyrosine ionization, as expected. (3) There are slight changes in the frequency and/or intensity of tryptophan bands which are suggestive of disruption of the internal H bond to a heme propionate group in both state II and state V.

Acknowledgments

We thank Professor Robert A. Pascal, Jr., and Ded Shih Huang for carrying out the SDS–acrylamide gel electrophoresis and Dr. John Eng for help in obtaining the far-UV absorption spectra.

Registry No. Cyt *c*, 9007-43-6.

References

Babul, J., & Stellwagen, E. (1972) *Biochemistry 11*, 1195–1200.

Carey, P. R. (1982) *Biochemical Applications of Raman and Resonance Raman Spectroscopies*, pp 71–98, Academic Press, New York.

Cohen, J. S., & Hayes, M. B. (1974) *J. Biol. Chem. 249*, 5472–5477.

Copeland, R. A., Dasgupta, S., & Spiro, T. G. (1985) *J. Am. Chem. Soc. 107*, 3370–3371.

Dickerson, R. E., & Timkovick, R. (1975) *Enzymes, 3rd Ed. 2*, 397–547.

Dickerson, R. E., Takano, T., Eisenberg, D., Kallai, O. B., Samson, L., Copper, A., & Margoliash, E. (1971) *J. Biol. Chem. 246*, 1511–1535.

Drew, H. R., & Dickerson, R. E. (1978) *J. Biol. Chem. 253*, 8420–8427.

Fodor, S. P. A., Rava, R. P., Hayes, T. R., & Spiro, T. G. (1985) *J. Am. Chem. Soc. 107*, 1520–1529.

Frushour, B. G., & Koenig, J. L. (1975) in *Advances in Infrared and Raman Spectroscopy* (Clark, R. J. H., & Hester, R. E., Eds.) Vol. I, pp 35–97, Heyden and Sons, New York.

Glasoe, P. K., & Long, F. A. (1960) *J. Phys. Chem. 64*, 188.

Harada, I., Sugawara, Y., Matsuura, H., & Shimanouchi, T. (1975) *J. Raman Spectrosc. 4*, 91–98.

Hudson, B., & Mayne, L. (1984) *Methods Enzymol.* (in press).

Johnson, C. R., Ludwig, M., O'Donnell, S., & Asher, S. A. (1984) *J. Am. Chem. Soc. 106*, 5008–5010.

Laemmeli, U. K. (1970) *Nature (London) 227*, 680–685.

Lambeth, D. O., Campbell, K. L., Zand, R., & Palmer, G. (1973) *J. Biol. Chem. 248*, 8130–8136.

Land, E. J., & Swallow, A. J. (1971) *Arch. Biochem. Biophys. 145*, 365–372.

Land, E. L., & Swallow, A. J. (1974) *Biochim. Biophys. Acta 368*, 86–96.

Moore, G. R., & Williams, R. J. P. (1980) *Eur. J. Biochem. 103*, 533–541.

Rava, R. P., & Spiro, T. G. (1984) *J. Am. Chem. Soc. 106*, 4062–4064.

Rava, R. P., & Spiro, T. G. (1985a) *J. Chem. Phys. 89*, 1856–1861.

Rava, R. P., & Spiro, T. G. (1985b) *Biochemistry 24*, 1861–1865.

Rosenheck, K., & Doty, P. (1961) *Proc. Natl. Acad. Sci. U.S.A. 47*, 1775–1785.

Saito, I., Sugiyama, H., Yamamoto, A., Muramatsu, S., & Matsuura, T. (1984) *J. Am. Chem. Soc. 106*, 4286–4287.

Schejter, A., Lanir, A., Vig, I., & Cohen, J. S. (1978) *J. Biol. Chem. 253*, 3768–3770.

Siamwiza, M. N., Lord, R. C., Chen, M. C., Takamatsu, T., Harada, I., Matsuura, H., & Shimanouchi, T. (1975) *Biochemistry 14*, 4870–4876.

Spiro, T. G. (1983) in *The Porphyrins, Part II* (Lever, A. B. P., & Gray, H. B., Eds.) pp 89–159, Addison-Wesley, Reading, MA.

Spiro, T. G., & Gaber, B. P. (1977) *Annu. Rev. Biochem. 46*, 553–572.

Sugawara, Y., Harada, I., Matsuura, H., & Shimanouchi, T. (1978) *Biopolymers 17*, 1405–1421.

Suzuki, S., Iwashita, Y., Shimanouchi, T., & Tsuboi, M. (1966) *Biopolymers 4*, 337–350.

Swanson, R., Trus, B. L., Mandel, N., Mandel, G., Kallai, O. B., & Dickerson, R. E. (1977) *J. Biol. Chem. 252*, 759–775.

Takano, T., Trus, B. L., Mandel, N., Mandel, G., Kallai, O. B., Swanson, R., & Dickerson, R. E. (1977) *J. Biol. Chem. 252*, 776–785.

Takesada, H., Nakanishi, M., Hirakawa, A. Y., & Tsuboi, M. (1976) *Biopolymers 15*, 1929–1938.

Theorell, H., & Åkkeson, Å. (1941) *J. Am. Chem. Soc. 63*, 1812–1818.

Vesterberg, O. (1971) *Biochim. Biophys. Acta 243*, 345–348.

Wharton, D. C., & Tzagaloff, A. (1967) *Methods Enzymol. 10*, 245–246.

Williams, R. W. (1983) *J. Mol. Biol. 166*, 581–603.

Wooten, J. B., Cohen, J. S., Vig, I., & Schejter, A. (1981) *Biochemistry 20*, 5394–5402.

Yoshikawa, S., Choc, M. G., O'Toole, M. C., & Caughey, W. S. (1977) *J. Biol. Chem. 252*, 5498–5508.

Ziegler, L. D., & Hudson, B. (1984) *J. Phys. Chem. 88*, 1110–1116.